

REGULAR ARTICLE

Synthesis, X-ray structure and theoretical investigation of 2-(2'-quinoly)benzimidazole metal complexes

FERIEL AOuatef SAHKI^a, LYAMINE MESSAADIA^b, HOCINE MERAZIG^a,
AISSA CHIBANI^a, ABDELMALEK BOURAIOU^{a,*} and SOFIANE BOUACIDA^{a,c}

^aUnité de Recherche de Chimie de l'Environnement et Moléculaire Structurale, Université des Frères
Mentouri, Constantine 25000, Algérie

^bLaboratoire Énergétique Appliquée et Matériaux, Université de Jijel, 18000 Jijel, Algérie

^cDépartement des sciences de la matière, Université Oum El Bouaghi, 04000, Oum El Bouaghi, Algérie
Email: bouraiou.abdelmalek@yahoo.fr

MS received 27 June 2016; revised 11 November 2016; accepted 15 November 2016

Abstract. Synthesis, characterization and DFT analysis of 2-(1*H*-benzo[d]imidazol-2-yl)quinoline (BQ) and its cobalt and manganese coordination compounds {Co(DMF)(BQ)Cl₂} and {Mn(DMF)(BQ)Cl₂} have been described. The ligand, 2-(1*H*-benzo[d]imidazol-2-yl)quinoline (BQ) crystallizes in non-centrosymmetric monoclinic crystal system with cell parameters $a = 12.9280(4) \text{ \AA}$, $b = 7.9429(3) \text{ \AA}$, $c = 25.8478(9) \text{ \AA}$, $\alpha = \gamma = 90^\circ$, $\beta = 103.005(2)^\circ$. {Co(DMF)(BQ)Cl₂} and {Mn(DMF)(BQ)Cl₂} crystallized in triclinic space group P-1. The metal(II) environment exhibits trigonal bipyramidal coordination. These complexes show presence of N–H...Cl, C–H...Cl hydrogen bonds and strong intramolecular C–H...O interactions. The structure parameters were calculated and they are in good agreement with those observed experimentally. Theoretically calculated frontier molecular orbitals (HOMO–LUMO) of the complexes and their energies indicate intermolecular charge transfer and delocalization of electron density within the molecule.

Keywords. Quinoline; benzimidazole; metal complexes; x-ray structure; electronic structure.

1. Introduction

Nitrogen-based ligands are extensively studied as complexes with many metal ions such as cobalt and manganese.^{1,2} Coordination complexes based on nitrogen donor chelate ligands and cobalt or manganese ions, having a number of available oxidation states, have attracted great attention because of their potential applications in various fields of human interest such as antitumor,^{3,4} antiviral,^{5,6} antifungal and antibacterial^{7,8} and antioxidant^{9,10} drugs. In addition to the biological importance, diverse catalytic^{11,12} and magnetic properties^{13,14} of such compounds have been explored.

Following our previous works related to the use of benzazole thioether as ligand for new coordination complexes,^{15,16} we report herein new manganese and cobalt complexes containing a polydentate ligand, by combination of quinoline and benzimidazole fragments. In addition, density functional theory calculations were used for determining the electronic structures, geometrical parameters, bonding analysis and reproducing efficiently the experimental structures.

2. Experimental

2.1 General considerations

All chemicals, reagents and solvents were of analytical grade, purchased and used as received. ¹H-NMR and ¹³C-NMR spectra were recorded on Bruker Avance DPX250 spectrometers. The melting point was determined using an Electrothermal IA9100 digital melting point apparatus. UV spectra were recorded on UV/VIS Spectrophotometer Optizen 1220. IR spectra were recorded on Shimadzu FT/IR-8201 PC spectrophotometer. Powder X-ray diffraction data were collected on a PANalytical X'Pert PRO X-ray powder diffractometer at room temperature. The 2θ scan range was 5–60°, with a step size of 0.007°. Microanalysis was performed in Perkin Elmer Elemental Analyzer 2400/II.

2.2 Synthesis of 2-(1*H*-benzo[d]imidazol-2-yl)quinoline (BQ)

10 mmol of phenylene diamine was added to a suspension of quinaldic acid (10 mmol) in 1 g of polyphosphoric acid. The mixture was heated at 160°C for 24 h. After completion of the reaction, water was added and the precipitate that formed was filtered, washed with H₂O (2 × 50 mL). The residue was suspended in 20 mL of NaOH (5 M), then filtered to afford the desired product. Yield 92%; Yellow solid; M.p.:

*For correspondence

85–88°C (Literature¹⁷: 93–95°C); UV–Vis (MeOH, $\lambda_{\text{max}}/\text{nm}$): 286, 308, 322, 336, 350; IR (KBr, cm^{-1}): 3047, 1654, 1596, 1566, 1500, 1411, 1319, 1238, 1141, 829, 748; ¹H NMR (250.13 MHz, CDCl_3) δ : 11.21 (s, 1H), 8.64–7.24 (m, 10H).

2.3 Preparation of complexes

2.3a Preparation of $\{\text{Co}(\text{DMF})(\text{BQ})\text{Cl}_2\}$ (1): A solution of 238 mg of $\text{CoCl}_2 \cdot 6\text{H}_2\text{O}$ (1 mmol) and 245 mg (1 mmol) of 2-(1H-benzo[d]imidazol-2-yl)quinoline (BQ) in 10 mL of MeOH was stirred for 18 h at room temperature. The green precipitate that formed was filtered and dried *in vacuo*. Yield 87%; M.p.: 205–210°C; UV–Vis (MeOH, $\lambda_{\text{max}}/\text{nm}$): 288, 310, 322, 336; IR (KBr, cm^{-1}): 3409, 3070, 1593, 1504, 1434, 1326, 1153, 837, 752. Anal. calcd. (%) for $\text{Co}(\text{BQ})\text{Cl}_2 \cdot \text{H}_2\text{O}$ ($\text{C}_{16}\text{H}_{13}\text{Cl}_2\text{CoN}_3\text{O}$): C 48.88, H 3.33, N 10.69, found (%): C 48.93, H 3.28, N 10.81. The crude product was recrystallized in DMF.

2.3b Preparation of $\{\text{Mn}(\text{DMF})(\text{BQ})\text{Cl}_2\}$ (2): A solution of 198 mg of $\text{MnCl}_2 \cdot 4\text{H}_2\text{O}$ (1 mmol) and 245 mg (1 mmol) of 2-(1H-benzo[d]imidazol-2-yl)quinoline (BQ) in 10 mL of MeOH was stirred at room temperature for 18 h. The light yellow precipitate that formed was filtered and dried *in vacuo*. Yield 78%; M.p.: 210–213°C; UV–Vis (MeOH, $\lambda_{\text{max}}/\text{nm}$): 288, 308, 322, 335; IR (KBr, cm^{-1}): 3436, 3058, 1596, 1504, 1431, 1323, 1149, 837, 756. Anal. calcd. (%) for $\text{Mn}(\text{BQ})_2\text{Cl}_2 \cdot \text{MeOH}$ ($\text{C}_{33}\text{H}_{26}\text{Cl}_2\text{MnN}_6\text{O}$): C 61.12, H 4.04, N 12.96, found (%): C 61.40, H 3.91, N 13.57. The crude product was recrystallized in DMF.

2.4 X-ray crystallography

The crystal was coated with Paratone oil and mounted on loops for data collection. X-ray data were collected with a Bruker Apex II CCD area detector diffractometer with a graphite-monochromated Mo-K α radiation source (0.71073 Å) at 298 K. The reported structure was solved by direct methods with SIR2002¹⁸ to locate all the non-H atoms which were refined anisotropically with SHELXL97¹⁹ using full-matrix least-squares on F^2 procedure from within the WinGX²⁰ suite of software used to prepare the material for publication. All absorption corrections were performed with the SADABS program.²¹ All the H atoms were placed in the calculated positions and constrained to ride on their parent atoms, except for H atoms of water molecule which were located in a difference map and their positions were refined isotropically with O–H distance restraints of 0.85 (2) Å and with $\text{Uiso}(\text{H}) = 1.2 \text{Ueq}(\text{O})$. Crystal data, structure refinement parameters, selected angles, bond lengths and some intra- and intermolecular interactions, hydrogen bonds for compounds BQ, $\{\text{Co}(\text{DMF})(\text{BQ})\text{Cl}_2\}$ (1) and $\{\text{Mn}(\text{DMF})(\text{BQ})\text{Cl}_2\}$ (2) are listed in Tables 1–3.

2.5 Computational studies

All the computational studies were carried out using the Gaussian 09 package²² and the Gauss-View molecular visualization program.²³ Density functional theory (DFT) methods using the combination of the Becke exchange functional²⁴ and the vp86 non-local correlation functional²⁵ combined with the 6-31G (p, d) basis set were utilized to determine the quantum chemical parameters for the title compounds, such as geometrical parameters, E_{HOMO} , E_{LUMO} , ΔE (energy gap) and dipole moment (μ).

3. Results and Discussion

3.1 Synthesis

2-(1H-benzo[d]imidazol-2-yl)quinoline (BQ) was synthesized following a literature procedure starting from phenylene diamine and quinaldic acid.²⁶ The complexes **1** and **2** were prepared as description in Scheme 1. The ligand (BQ) was stirred in MeOH with MCl_2 overnight at room temperature. The solid M(II) complexes was filtered off and dried. These are very stable in the air. The M(II) complexes are soluble in DMF and DMSO but insoluble in water and other organic solvents, such as methanol. To verify the phase purity of the prepared complexes, the PXRD pattern was recorded. The diffractograms indicated that both complexes are pure phases. The obtained complexes were recrystallized in DMF (Scheme 1).

3.2 Crystal structures

The ligand (BQ) and the two obtained complexes were recrystallized and suitable crystals of BQ, **1** and **2** were grown in DMF solution. It should be noted that during the recrystallisation step, the DMF molecule coordinates through O atoms to the metallic atom in both M(II) complexes. The X-ray crystallographic analysis confirmed their respective structures and the refined X-ray crystal structures are shown in Figure 1. Crystal data and structural details of the prepared complexes are presented in Table 1.

3.2a Crystal structure of ligand BQ: The ligand 2-(1H-benzo[d]imidazol-2-yl)quinoline (BQ) crystallizes in non-centrosymmetric monoclinic crystal system (space group Cc). The asymmetric unit contains two co-crystallized water molecules and two ligands, crystallographically independent (molecules A and B). Each molecule consists of a benzimidazole unit connected to quinolyl moiety. The C–N bonds lengths values are, N(1A)–C(1A) (1.379(5) Å), N(1A)–C(9A) (1.308(4) Å), N(2A)–C(10A) (1.373(4) Å), N(2A)–C(11A) (1.371(5) Å),

Table 1. Crystallographic data and refinement parameters for BQ, complexes **1** and **2**.

	BQ	{Co(DMF)(BQ)Cl ₂ } (1)	{Mn(DMF)(BQ)Cl ₂ } (2)
Formula	C ₁₆ H ₁₁ N ₃ , H ₂ O	C ₁₉ H ₁₈ Cl ₂ Co N ₄ O	C ₁₉ H ₁₈ Cl ₂ Mn N ₄ O
Formula weight	263.29	448.2	474.28
Crystal habit, color	Prism, Colorless	Prism, Blue	Prism, Colorless
Crystal system	Monoclinic	Triclinic	Triclinic
Space group	C c	P -1	P -1
a (Å)	12.9280(4)	8.5673(12)	8.6355(13)
b (Å)	7.9429(3)	10.7470(17)	10.8411(16)
c (Å)	25.8478(9)	12.1600(16)	12.1779(18)
α (°)	90	103.071(13)	104.473(7)
β (°)	103.005(2)	94.461(9)	93.532(7)
γ (°)	90	112.97(2)	113.324(6)
Volume (Å ³)	2586.12(16)	986.8(2)	997.0(3)
Z, Z'	4, 8	2, 2	2, 2
Density (calculated, g cm ⁻³)	1.352	1.508	1.480
Absorption coefficient (mm ⁻¹)	0.088	1.157	0.946
F(000)	1104	458	454
Crystal size (mm)	0.08 × 0.13 × 0.15	0.05 × 0.10 × 0.13	0.09 × 0.14 × 0.19
θ range for data collection (°)	3.23–30.54	3.42–31.16	3.40–36.23
Reflections collected	14330	14863	36453
Independent reflections	6562	5839	9496
R _{int}	0.0352	0.0530	0.0196
Reflections with I ≥ 2σ(I)	3757	3334	7273
Number of parameters	373	246	246
Goodness-of-fit on F ²	0.984	1.052	1.029
Final R indices [I ≥ 2σ(I)]	0.0591	0.0737	0.0348
R indices [all data]	R ₁ = 0.1145,	R ₁ = 0.1380, wR ₂ = 0.1825,	R ₁ = 0.0963, wR ₂ = 0.1068
Largest difference peak and hole (Å ⁻³)	wR ₂ = 0.1298,	1.185, -0.88	0.432, -0.248
CCDC deposition no.	CCDC 1455171	CCDC 1469612	CCDC 1455172

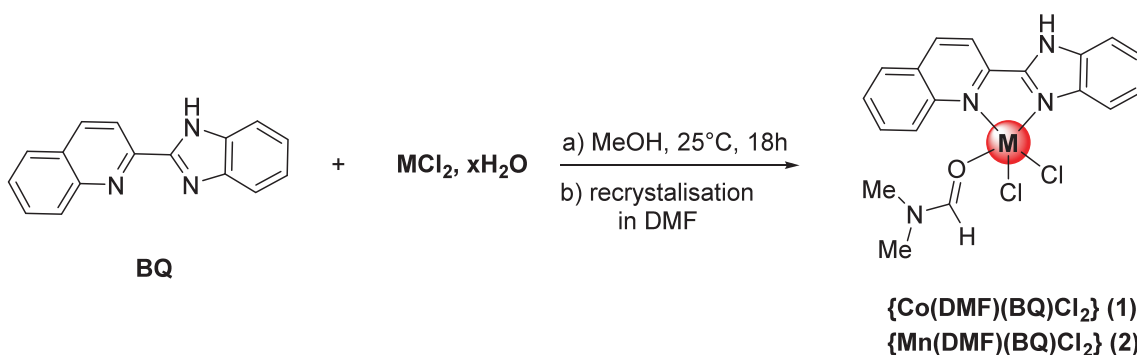
Table 2. Distances (Å) and angles (°) of hydrogen bond for BQ, complexes (**1**) and (**2**).

D–H...A	d(D–H)	d(H...A)	d(D–A)	D–H–A	Symmetry
BQ					
O1w–H1w...N1a	0.89(3)	2.24(4)	3.069(4)	156(3)	1/2+x, 1/2+y, z
O1w–H2w...N3b	0.86(3)	2.02(4)	2.808(4)	151(3)	x, y, z
O2w–H3w...O1w	0.92(3)	2.50(4)	2.948(4)	110(3)	x, y, z
O2w–H3w...N1b	0.92(3)	2.23(4)	3.035(4)	147(3)	x, 1+y, z
O1w–H4w...N3a	0.88(3)	1.94(4)	2.811(4)	169(4)	x, y, z
N2a–H21a...O2w	0.86	1.9500	2.766(4)	159.00	-1/2+x, -1/2+y, z
N2b–H21b...O1w	0.86	1.9500	2.771(4)	159.00	x, y, z
{Co(DMF)(BQ)Cl ₂ } (1)					
N3–H3n...Cl2	0.86	2.3300	3.160(5)	161.00	2-x, 1-y, -z
C12–H12...O21	0.93	2.5400	3.160(5)	123.00	x, y, z
C22–H22a...Cl1	0.96	2.7200	3.643(9)	161.00	2-x, 2-y, 1-z
{Mn(DMF)(BQ)Cl ₂ } (2)					
N3–H3n...Cl1	0.86	2.3200	3.149(1)	160.00	1-x, 1-y, -z
C12–H12...O21	0.93	2.5700	3.189(2)	124.00	x, y, z
C22–H22a...Cl2	0.96	2.7200	3.633(2)	160.00	1-x, 2-y, 1-z
C23–H23c...O21	0.96	2.4400	2.772(3)	100.00	x, y, z

N(3A)–C(10A) (1.308(4) Å), N(3A)–C(16A) (1.370 (5) Å) (molecule A), N(1B)–C(1B) (1.379(5) Å), N (1B)–C(9B) (1.317(4) Å), N(2B)–C(10B) (1.347(5) Å), N(2B)–C(11B) (1.390(5) Å), N(3B)–C(10B) (1.317(4) Å), N(3B)–C(16B) (1.397(5) Å) (molecule B), which indicate partial double bond character (Table 2). Bond

Table 3. Selected bond lengths (Å) and angles (°) for ligand BQ, complexes **1** and **2** with estimated standard deviations; theoretical structure parameters obtained by bvp86/6-31G(d, p) are given in parentheses.

Bond length/Bond angle	BQ(A)	BQ(B)	{Co(DMF)(BQ)Cl ₂ } (1)	{Mn(DMF)(BQ)Cl ₂ } (2)
C10-N2	1.373(4)	1.347(5) (1.336)	1.323(6) (1.336)	1.3249(13) (1.327)
C10-N3	1.308(4)	1.317(4) (1.309)	1.354(6) (1.346)	1.3488(13) (1.3469)
C16-N3	1.370(5)	1.397(5) (1.390)	1.375(6) (1.390)	1.3808(15) (1.3909)
C9-C10	1.477(5)	1.465(5) (1.487)	1.467(6) (1.487)	1.4685(14) (1.487)
N1-M		–	2.275(4) (2.275)	2.3781(9) (2.388)
N2-M		–	2.042(4) (2.009)	2.1772(9) (2.024)
M1-021		–	2.092(4) (2.092)	2.1662(9) (2.166)
M-Cl1		–	2.2717(15) (2.271)	2.4249(4) (2.424)
M-Cl2		–	2.3389(15) (2.338)	2.3421(4) (2.342)
N1-C9-C10	116.8(3)	116.1(3) (124.2)	112.8(4) (113.3)	113.99(9) (113.36)
N2-C10-N3	112.7(3)	114.0(4) (110.3)	113.1(4) (110.34)	112.48(9) (110.65)
N1-M1-N2		–	75.94(14) (75.94)	73.04(3) (73.70)
N2-M1-Cl1		–	117.09(12) (119.36)	117.02(3) (119.42)
Cl1-M1-Cl2		–	118.82(6) (118.81)	119.364(17) (119.364)

**Scheme 1.** Synthesis of **1** and **2**.

angles for N(1A)–C(9A)–C(10A) and for N(2A)–C(10A)–N(3A) are 116.8 (3)° and 112.7 (3)°, respectively, and the bond angle N(2A)–C(10A)–C(9A) is 120.9 (3)° (Table 1). Both molecules A and B are almost planar and parallel which form a dihedral angle of 0.93(2)°. The crystal packing can be described as alternating double layers in zigzag manner along the b axis (at b=0 and b=1/2) parallel to (010) plane (Figure 2). These layers are connected together

with water molecule *via* O–H...N and N–H...O hydrogen bonding interactions resulting in the formation of three dimensional network. Hydrogen bond between amine moieties and water molecule form a chain with $D_1^1(2)$ graph set motif,²⁷ when water molecule acts as acceptor as well as donor. Additional hydrogen-bonding parameters are listed in Table 2. The packing is consolidated by slipped $\pi - \pi$ stacking with centroid to centroid distance of 3.777(2) Å

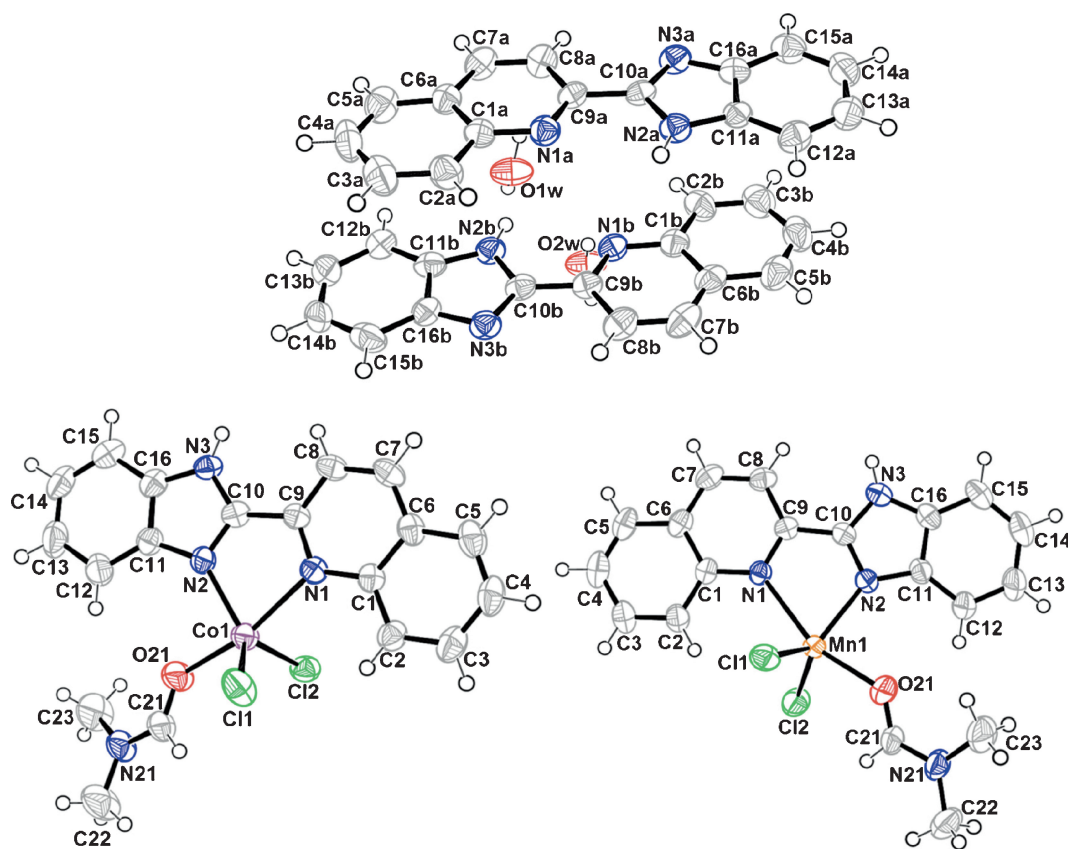


Figure 1. Oak Ridge thermal ellipsoid plots (ORTEP) of the molecular structures of BQ, $\{\text{Co}(\text{DMF})(\text{BQ})\text{Cl}_2\}$ (**1**), and $\{\text{Mn}(\text{DMF})(\text{BQ})\text{Cl}_2\}$ (**2**) in the crystal and atom numbering scheme adopted (displacement ellipsoids at the 50% probability level; H atoms with arbitrary radii).

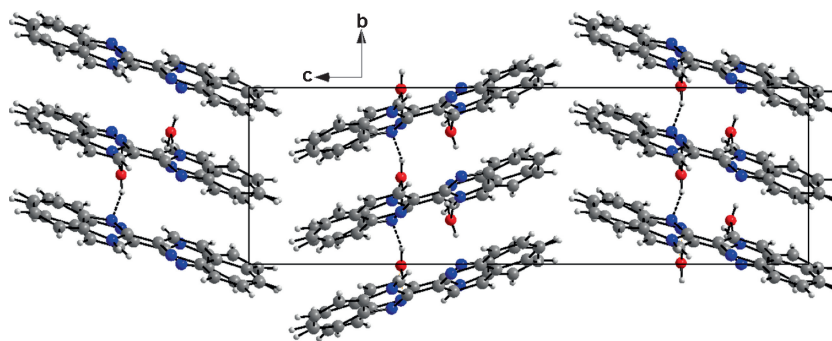


Figure 2. Diagram packing of BQ viewed along the *a* axis showing layers in zigzag parallel to (010) plane which are connected with water molecule with N–H...O and O–H...N hydrogen bonds.

to 3.878(2) Å. All these interactions link the molecule within the layers and also link layers together and reinforce the cohesion of the organic structure.

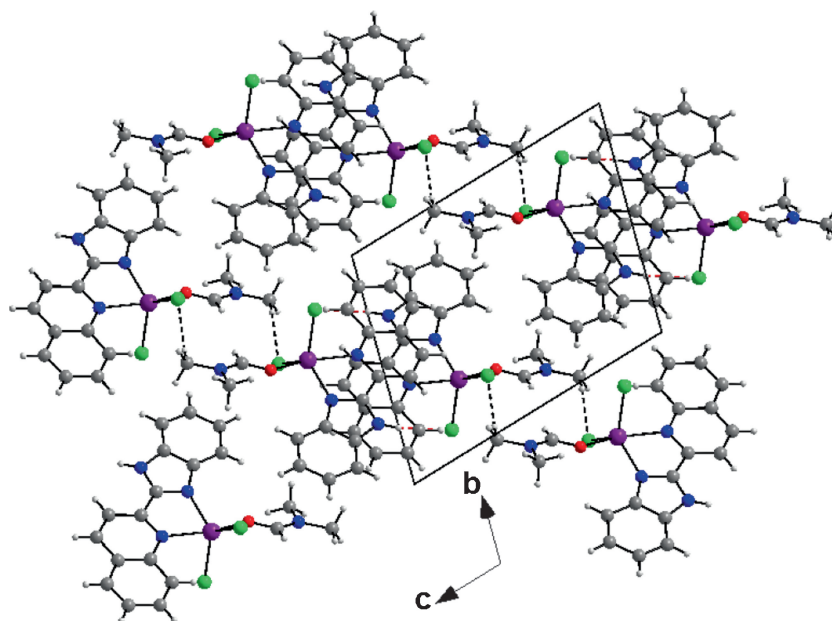
3.2b Crystal structure of complexes $\{\text{Co}(\text{DMF})(\text{BQ})\text{Cl}_2\}$ (1**) and $\{\text{Mn}(\text{DMF})(\text{BQ})\text{Cl}_2\}$ (**2**):** The compounds **1** and **2** crystallized in triclinic space group P-1. Selected bond distances and bond angles for both compounds are listed in Tables 3 and 4. Both complexes are five-coordinated (Figure 1, Table 1). The metal ion is surrounded by two N-donor atoms of the

2-(1*H*-benzo[*d*]imidazol-2-yl)quinoline (BQ) ligand, two chloride ions and one coordinated DMF molecule (Figure 1). Each complex contains one organic ligand that contain two rings, N1, C1–C9 (quinoline ring) and N2, N3, C10–C16 (benzimidazole ring).

The metal (II) environment exhibits Trigonal bipyramidal coordination. The bond lengths around the metal centers are in the range of 2.042(4)–2.3781(13) Å (N–M), 2.2717(15)–2.4249(4) Å (Cl–M), 1.237(7)–1.2383(16) Å (O–M). Bond angles for N1–Co1–Cl1, N1–Mn1–Cl1, Cl1–Co1–O21 and for Cl1–Mn1–O21

Table 4. Calculated quantum chemical parameters of the BQ and complexes **1** and **2** calculated at DFT at the bvp86/6-31G (d, p) level.

Parameters	BQ	{Co(DMF)(BQ)Cl ₂ } (1)	{Mn(DMF)(BQ)Cl ₂ } (2)
Total energy (Hartree)	−780.57620552	−3332.4023263	−3100.6407187
E_{HOMO} (eV)	−5.0197	−4.569	−4.628
E_{LUMO} (eV)	−2.736	−3.773	−3.556
ΔE_{H-L} (eV)	2.283	0.796	1.072
μ (debye)	4.5409	8.6330	8.3973

**Figure 3.** Diagram packing of **1** showing layers parallel to (1-10) plane and C–H...Cl interactions in black ($R_2^2(12)$).

are 98.46(10)°, 88.53 (2)°, 97.32 (16)° and 90.64(3)°, respectively. Bond lengths and angles are comparable to those reported previously and are in the expected range.^{28,29}

The crystal packing for both complexes can be described as alternating layers parallel to (1-10) plane (Figures 3 and 4). In these layers, the arrangement of each molecule induces strong π – π stacking intermolecular interaction. The shortest centroid–centroid distances are 3.458(3) and 3.465(1) Å for Co and Mn complex, respectively. Also these complexes present N–H...Cl and C–H...Cl hydrogen bonds forming chain and ring, respectively, with $D_1^1(2)$ and $R_2^2(12)$ graph set motif.²⁷ Strong intramolecular interactions of C–H...O are found in the crystal packing. (Figures 3 and 4, Table 2).

3.3 Computational details

3.3a Geometrical structure: The optimized structure parameters (bond lengths and angles) for title complexes were calculated using the density functional theory (DFT)/ bvp86/6-31G (p, d) method. The structural

parameters such as bond length and bond angles found from the crystal structures are compared with those of optimized geometries. Table 3 summarizes some selected geometrical parameters of the investigated compounds. In general, the obtained results were found to be in good agreement with experimental values, except some bond lengths, such as C9–C10 and N2–M (M=Co, Mn). For example, deviations between calculated and experimental N2–M bonds distances are 0.01 Å for **BQ(A)**, 0.022 Å for **BQ(B)**, 0.020 Å for complex **1** and 0.018 Å for complex **2**, respectively. However, for bond angles, we can see that the variations are shorter and longer between the experimental and optimized values due to intermolecular interactions by quinoline with the metal. Moreover, we note that the experimental results belong to the solid state and the theoretical calculations belong to the gas phase.

3.3b Frontier molecular orbitals (HOMO–LUMO) analysis: The optimization of molecular geometry of title compounds in the gas phase was calculated in

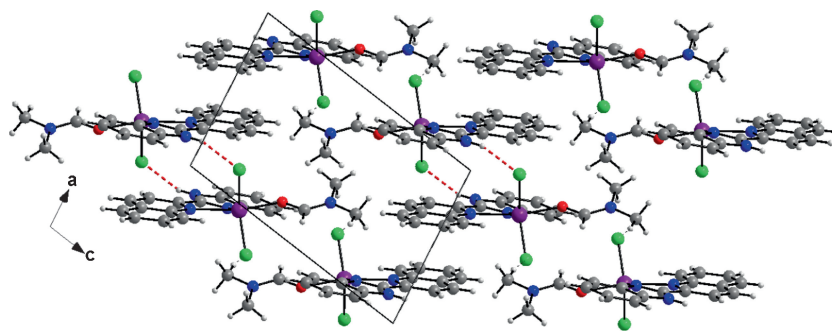


Figure 4. Diagram of packing of **1** viewed along *a* axis showing N–H...Cl interactions in red ($D_1^1(2)$).

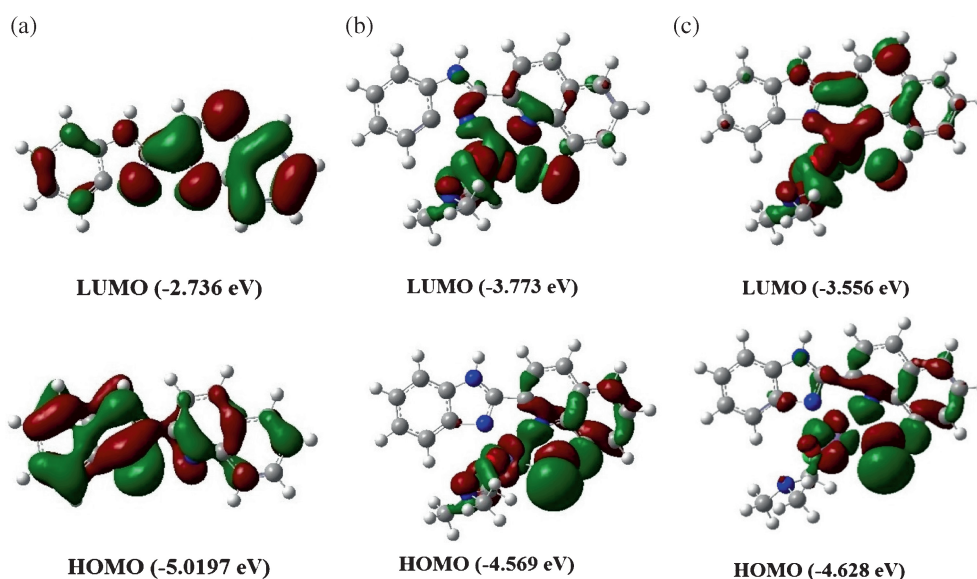


Figure 5. Frontier molecular orbitals of compounds (a) ligand BQ, (b) complex {Co(DMF)(BQ)Cl₂} (**1**), and (c) complex {Mn(DMF)(BQ)Cl₂} (**2**).

order to study the stability of the total energy and the energy gap between the frontier molecular orbitals ($\Delta E_{H-L} = E_{HOMO} - E_{LUMO}$) using the density functional theory (DFT) at bvp86/6-31G (d, p) level. The frontier orbital gap helps to characterize the chemical reactivity and kinetic stability of the molecules. A molecule with a small frontier orbital gap is more polarizable and is generally associated with a high chemical reactivity, low kinetic stability and is also called as a soft molecule.³⁰ The HOMO represents ability to donate an electron and LUMO represents the ability to accept an electron. Table 4 shows the total energy, E_{LUMO} , E_{HOMO} and ΔE_{H-L} energy gap of both complexes **1**, **2** and Ligand BQ. The calculations indicate that the complex **1** has lower value of total energy and energy gap (ΔE_{H-L}) than complex **2**. Therefore, complex **1** is more reactive than **2**. The 3D plots of the frontier molecular orbitals HOMO and LUMO for title compounds are illustrated in Figure 5. As can be seen in Figure 5, the HOMO for complexes **1** and **2** are mainly located over

the chlorine (Cl), azote (N1, N21), oxygen (O21) and cobalt (Co) atoms, with contributions on the quinoline ring BQ(B). The LUMO is mostly centered in chlorine (Cl), azote (N1, N21, N2, N3), oxygen (O21) and cobalt (Co) atoms, with slight contribution of quinoline ring BQ(B). In the case of ligand BQ, the HOMO is delocalized almost over the whole π -conjugated system, while the LUMO, and is also delocalized over the whole molecule. The LUMO and HOMO energy gap for the complex **1** equal to 0.796 eV, which is lower than that of complex **2** (1.072 eV) and ligand BQ (2.283 eV), reflecting intermolecular charge transfer and delocalization of electron density within the molecule.³¹ Therefore, it is clear that the complex **1** is more reactive and more polar than complex **2** and ligand BQ.

4. Conclusions

In summary, this paper describes the synthesis, single crystal X-ray diffraction analysis and DFT studies of

2-(2'-quinolyl)benzimidazole and Co and Mn complexes. The complexes were synthesized using a simple method. Single crystal X-ray diffraction analysis of the studied complexes reveals a trigonal bipyramidal coordination of the metal(II) environments. These complexes present N–H...Cl, C–H...Cl and C–H...O interactions in the crystal packing. The theoretical and experimental bond lengths and angles are in good agreement with each other. Theoretically calculated frontier molecular orbitals (HOMO-LUMO) of both complexes suggest intermolecular charge transfer and delocalization of electron density within the molecule. The accuracy of the results also predicts that the DFT studies performed at bvp86/6-31G (p, d) level is an appropriate quantum chemical method for reproducing efficiently the experimental structures.

Supplementary Information (SI)

Crystallographic information for all the compounds have been deposited with the Cambridge crystallographic data center, (CCDC) as supplementary publications CCDC 1455171, 1469612 and 1455172. The electronic Supplementary Information is available at www.ias.ac.in/chemsci.

Acknowledgements

We are grateful to the Ministère de l'Enseignement Supérieur et de la Recherche Scientifique – Algérie (MESRS) for financial support.

References

- Hashihayata T, Ito Y and Katsuki T 1996 Enantioselective epoxidation of 2,2-dimethylchromenes using achiral Mn-Salen complex as catalyst in the presence of chiral amine *Synlett* 1079
- Soliman S M, Abu Youssef M A M, Albering J and El Faham A 2015 Molecular structure and DFT investigation on new cobalt(II) chloride complex with super-base guanidine type ligand *J. Chem. Soc.* **127** 2137
- Lv J, Liu T, Cai S, Wang X, Liu L and Wang Y 2006 Synthesis, structure and biological activity of cobalt(II) and copper(II) complexes of valine-derived schiff bases *J. Inorg. Biochem.* **100** 1888
- Zhong X, Wei H-L, Liu W-S, Wang D-Q and Wang X 2007 The crystal structures of copper(II), manganese(II), and nickel(II) complexes of a (Z)-2-hydroxy-N'-(2-oxoindolin-3-ylidene) benzohydrazide-potential antitumor agents *Bioorg. Med. Chem. Lett.* **17** 3774
- Takeuchi T, Böttcher A, Quezada C M, Meade T J and Gray H B 1999 Inhibition of Thermolysin and Human-Thrombin by Cobalt(III) Schiff Base Complexes *Bioorg. Med. Chem.* **7** 815
- Rogolino D, Carcelli M, Bacchi A, Compari C, Contardi L, Fisicaro E, Gatti A, Sechi M, Stevaert A and Naesens L 2015 A versatile salicyl hydrazonic ligand and its metal complexes as antiviral agents *J. Inorg. Biochem.* **150** 9
- Maghami M, Farzaneh F, Simpson J, Ghiasi M and Azarkish M 2015 Synthesis, crystal structure, antibacterial activity and theoretical studies on a novel mononuclear cobalt(II) complex based on 2,4,6-tris(2-pyridyl)-1,3,5-triazine ligand *J. Mol. Struct.* **1093** 24
- Kani I, Altier Ö and Güven K 2016 Mn(II) complexes with bipyridine, phenanthroline and benzoic acid: Biological and catalase-like activity *J. Chem. Sci.* **128** 523
- Dimiza F, Papadopoulos A N, Tangoulis V, Psycharis V, Raptopoulou C P, Kessissoglou D P and Psomas G 2012 Biological evaluation of cobalt(II) complexes with non-steroidal anti-inflammatory drug naproxen *J. Inorg. Biochem.* **107** 54
- Bernard A-S, Giroud C, Ching H Y V, Meunier A, Ambike V, Amatore C, Collignon G M, Lemaître F and Policar C 2012 Evaluation of the anti-oxidant properties of a SOD-mimic Mn-complex in activated macrophages *Dalton Trans.* **41** 6399
- Miura K and Katsuki T 1999 Dynamic Control of Ligand Conformation: Asymmetric Epoxidation Using Achiral (Salen)manganese(III) Complex *Synlett* 783
- Yamada T, Ikeno T, Sekino H and Sato M 1999 Optically Active Aldiminato Cobalt(II) Complexes as Efficient Catalysts for Enantioselective Cyclopropanation of Styrenes with Diazoacetates *Chem. Lett.* **28** 719
- Alam R, Pal K, Shaw B K, Dolai M, Pal N, Saha S K and Ali M 2016 Synthesis, structure, catalytic and magnetic properties of a pyrazole based five coordinated di-nuclear cobalt(II) complex *Polyhedron* **106** 84
- Yuan J, Wang X, Liu M-J and Kou H-Z 2016 Manganese (III) complexes derived from 1-(2-hydroxybenzamido)-2-((2-hydroxy-3-methoxybenzylidene)amino)ethane: Synthesis, structure and magnetic properties *Inorg. Chim. Acta* **449** 69
- Mezhoud B, Bouchouit M, Said M E, Messaadia L, Belfaitah A, Merazig H, Chibani A, Bouacida S and Bouraiou A 2016 Synthesis, X-ray structure and theoretical study of benzazole thioether and its zinc complex as corrosion inhibitors for steel in acidic medium *Res. Chem. Intermed.* **42** 7447
- Bouchouit M, Benzerka S, Bouraiou A, Merazig H, Belfaitah A and Bouacida S 2015 Crystal structure of {bis[(1H-benzimidazol-2-yl-κN³)methyl]sulfane} dichloridomercury(II) *Acta Cryst.* **E71** m253
- Mamedov V A, Saifina D F, Gubaidullin A T, Ganieva V R, Kadyrova S F, Rakov D V, Rizvanov I K and Sinyashin O G 2010 Acid-catalyzed rearrangement of 3-(β-2-aminostyryl)quinoxalin-2(1H)ones-a new and efficient method for the synthesis of 2-benzimidazol-2-ylquinolines *Tetrahedron Lett.* **51** 6503
- Burla M C, Caliandro R, Camalli M, Carrozzini B, Cascarano G L, De Caro L, Giacovazzo C, Polidori G and Spagna R 2005 SIR2004: An improved tool for crystal structure determination and refinement *J. Appl. Cryst.* **38** 381
- Sheldrick G M 2008 A short history of SHELX *Acta Cryst. A* **64** 112
- Farrugia L J 2012 WinGX and ORTEP for Windows: An update *J. Appl. Cryst.* **45** 849

21. Sheldrick G M 2002 SADABS (Bruker AXS Inc.: Madison, Wisconsin, USA)
22. Frisch M J, Trucks G W, Schlegel H B, Scuseria G E, Robb M A, Cheeseman J R, Scalmani G, Barone V, Mennucci B, Petersson G A, Nakatsuji H, Caricato M, Li X, Hratchian H P, Izmaylov A F, Bloino J, Zheng G, Sonnenberg J L, Hada M, Ehara M, Toyota K, Fukuda R, Hasegawa J, Ishida M, Nakajima T, Honda Y, Kitao O, Nakai H, Vreven T, Montgomery J A, Peralta Jr J E, Ogliaro F, Bearpark M, Heyd J J, Brothers E, Kudin K N, Staroverov V N, Keith T, Kobayashi R, Normand J, Raghavachari K, Rendell A, Burant J C, Iyengar S S, Tomasi J, Cossi M, Rega N, Millam J M, Klene M, Knox J E, Crossi J B, Bakken V, Adamo C, Jaramillo J, Gomperts R, Stratmann R E, Yazyev O, Austin A J, Cammi R, Pomelli C, Ochterski J W, Martin R L, Morokuma K, Zakrzewski V G, Voth G A, Salvador P, Dannenberg J J, Dapprich S, Daniels A D, Farkas O, Foresman J B, Ortiz J V, Cioslowski J and Fox D J 2009 *Gaussian 09*, Revision C.01; Gaussian Inc., Wallingford CT
23. Dennington R, Keith T and Millam J 2009 *GaussView* Version 5.0.9 (Semichem Inc.: Shawnee Mission KS)
24. Becke A D 1988 Density-functional exchange-energy approximation with correct asymptotic behavior *Phys. Rev. A* **38** 3098
25. Perdew J P 1986 Density-functional approximation for the correlation energy of the inhomogeneous electron gas *Phys. Rev. B* **33** 8822
26. Hisano T, Ichikawa M and Tsumoto K 1982 Synthesis of Benzoxazoles, Benzothiazoles and Benzimidazoles and Evaluation of Their Antifungal, Insecticidal and Herbicidal Activities *Chem. Pharm. Bull.* **30** 2996
27. Etter M C, MacDonald J C and Bernstein J 1990 Graph-set analysis of hydrogen-bond patterns in organic crystals *Acta Cryst. B* **46** 256
28. Min J, Zhang Q, Sun W, Cheng Y and Wang L 2011 Neutral copper(I) phosphorescent complexes from their ionic counter parts with 2-(2'-quinolyl)benzimidazole and phosphine mixed ligands *Dalton Trans.* **40** 686
29. Chen S Y, Guo Y C, Zhang L F, Feng Y Q, Zhang Y Y and Huaxue J 2013 Syntheses, Crystal Structures and Photoluminescence Properties of Cadmium(II) and Nickel(II) Complexes with 2-(2-Benzimidazolyl)quinoline *Chin. J. Struct. Chem.* **32** 643
30. Fleming I 1976 In *Frontier Orbitals and Organic Chemical Reactions* (New York: John Wiley) pp. 5–27
31. Bouchouit M, Elkouari Y, Messaadia L, Bouraiou A, Arroudj S, Bouacida S, Taboukhat S and Bouchouit K 2016 Synthesis, spectral, theoretical calculations and optical properties performance of substituted-azobenzene dyes *Opt. Quant. Electron.* **48** 178